HHS Public Access

Author manuscript

Pulm Pharmacol Ther. Author manuscript; available in PMC 2019 October 25.

Published in final edited form as:

Pulm Pharmacol Ther. 2019 April ; 55: 38–49. doi:10.1016/j.pupt.2019.01.007.

SUMOylation of Vps34 by SUMO1 promotes phenotypic switching of vascular smooth muscle cells by activating autophagy in pulmonary arterial hypertension

Yufeng Yao[a,1], **Hui Li**[a,1], **Xinwen Da**[a,1], **Zuhan He**[a], **Bo Tang**[a], **Yong Li**[a], **Changqing Hu**[a], **Chengqi Xu**[a], **Qiuyun Chen**[b,c,**], **Qing K. Wang**[a,b,c,d,*]

[a]Key Laboratory of Molecular Biophysics of the Ministry of Education, College of Life Science and Technology and Center for Human Genome Research, Huazhong University of Science and Technology, Wuhan, PR China

[b]Department of Cardiovascular and Metabolic Sciences, Lerner Research Institute, Cleveland Clinic, Cleveland, OH, 44195, USA

[c]Department of Molecular Medicine, CCLCM of Case Western Reserve University, Cleveland, OH, 44195, USA

[d]Department of Genetics and Genome Sciences, Case Western Reserve University School of Medicine, Cleveland, OH, 44106, USA

Abstract

Introduction: Pulmonary arterial hypertension (PAH) is a life-threatening disease without effective therapies. PAH is associated with a progressive increase in pulmonary vascular resistance and irreversible pulmonary vascular remodeling. SUMO1 (small ubiquitin-related modifier 1) can bind to target proteins and lead to protein SUMOylation, an important post-translational modification with a key role in many diseases. However, the contribution of SUMO1 to PAH remains to be fully characterized.

Methods: In this study, we explored the role of SUMO1 in the dedifferentiation of vascular smooth muscle cells (VSMCs) involved in hypoxia-induced pulmonary vascular remodeling and PAH *in vivo* and *in vitro*.

Results: In a mouse model of hypoxic PAH, SUMO1 expression was significantly increased, which was associated with activation of autophagy (increased LC3b and decreased p62), dedifferentiation of pulmonary arterial VSMCs (reduced α-SMA, SM22 and SM-MHC), and pulmonary vascular remodeling. Similar results were obtained in a MCT-induced PAH model.

*Corresponding author. Center for Human Genome Research, Huazhong University of Science and Technology, Wuhan, China. qkwang@hust.edu.cn, wangq2@ccf.org (Q.K. Wang). **Corresponding author. Department of Cardiovascular and Metabolic Sciences, Lerner Research Institute, Cleveland Clinic, Cleveland, OH, 44195, USA. chenq3@ccf.org (Q. Chen).

Author contributions

YY and QKW conceived and designed the study; YY, HL, YL, CH, ZH, BT, and XD performed experiments; YY, CH, QS, IX, QC and QKW analyzed data; YY and QKW drafted the manuscript; YY, Q.C. and QKW critically revised the manuscript; Q.C. and QKW supervised the study; All authors reviewed the manuscript.

[1]These authors contributed equally to this work.

Disclosures

The authors declare that they have no competing interests.

Overexpression of SUMO1 significantly increased VSMCs proliferation, migration, hypoxia-induced VSMCs dedifferentiation, and autophagy, but these effects were abolished by inhibition of autophagy by 3-MA in aortic VSMCs. Furthermore, SUMO1 knockdown reversed hypoxia-induced proliferation and migration of PASMCs. Mechanistically, SUMO1 promotes Vps34 SUMOylation and the assembly of the Beclin-1-Vps34-Atg14 complex, thereby inducing autophagy, whereas Vps34 mutation K840R reduces Vps34 SUMOylation and inhibits VSMCs dedifferentiation.

Discussion: Our data uncovers an important role of SUMO1 in VSMCs proliferation, migration, autophagy, and phenotypic switching (dedifferentiation) involved in pulmonary vascular remodeling and PAH. Targeting of the SUMO1-Vps34-autophagy signaling axis may be exploited to develop therapeutic strategies to treat PAH.

Keywords

Vps34; Beclin-1; Atg14

1. Introduction

Pulmonary arterial hypertension (PAH) is a lethal disease with a high mortality rate, and characterized by pulmonary vascular remodeling [1-4]. In hypoxia-induced PAH, pulmonary arterial vascular smooth muscle cells (PASMCs) undergo a contractile-to-synthetic phenotypic switching, a major cause underlying pulmonary vascular remodeling [3-5]. A contractile phenotype of vascular smooth muscle cells (VSMCs) is characterized by an increased expression level of a repertoire of markers, including α-smooth muscle-actin (α-SMA), SM22, and SM-MHC [6,7]. After vascular injury or pathological conditions, VSMCs undergo a transition from a contractile phenotype to a synthetic phenotype (dedifferentiation) with less expression levels of α-SMA, SM22, and SM-MHC, but increased proliferation [7,8]. In PAH, excessive proliferation of PASMCs and reduced apoptosis accelerate vascular remodeling [9]. However, the molecular mechanisms of pulmonary vascular remodeling in PAH are complicated and remain incompletely understood [10].

The ubiquitin system promotes important post-translational modifications of proteins, and targets the modified proteins for degradation [11]. Small ubiquitin-related modifier-1 (SUMO1) is a small protein (11.5 kDa) that belongs to the SUMO (small ubiquitin-like modifier) protein family [12,13]. SUMO1 is highly conserved among different species [14-17]. Previous studies showed that mitochondrial division or fission is significantly enhanced in patients with PAH [18]. Mitochondrial dynamics affects apoptosis, mitochondrial DNA stability, and the level of free oxygen and cellular oxidative stress responses, which can affect disease development [18-22]. Boucherat et al. showed that HSP90 was preferentially localized in the mitochondria of PAH-PASMCs in response to stress and regulated mitochondrial DNA content and repair capacity and bioenergetic functions involved in PAH-PASMCs proliferation [22]. Interestingly, Gamitrinib, a mitochondria-targeted HSP90 inhibitor, was shown to improve PAH in rat PAH models [22]. Study showed the SUMO protease SENP5 impacted mitochondrial morphology and metabolism [23]. Dynamin-related protein 1 (DRP1), which promotes mitochondrial fission

involved in PAH, is regulated by SUMO1, and a recent study showed that epigenetic upregulation of DRP1 adapter proteins MiD49 and MiD51 by miR-34a-3p was involved in the pathophysiology of PAH [20,24-26]. The main function of SUMO1 was to prevent proteasome-mediated degradation of proteins as a brake to ubiquitination [14,27]. SUMO1 is involved in SUMOylation of different proteins, and stabilizes SUMOylated proteins [28]. In addition to its role in protein stability, SUMO1 is also involved in nuclear transport, transcriptional regulation, and apoptosis [29-31].

Autophagy is an evolutionarily conserved cell catabolic process, which is induced by starvation or stress, and used by eukaryotic cells to degrade and recycle various damaged or long-lived proteins and dys-functional or superfluous organelles [32-36]. Many important cellular processes, including cell proliferation and apoptosis, are affected by autophagy [36-38]. Autophagy is activated in several human pulmonary diseases, such as obstructive pulmonary disease, idiopathic pulmonary fibrosis, and PAH [12,39-43]. In a rat monocrotaline (MCT) model for PAH, chloroquine (an autophagy inhibitor) inhibited the development of PAH by inhibiting proliferation and increasing apoptosis of PASMCs [44].

In the present study, we found that SUMO1 expression was significantly increased in both hypoxia-induced and MCT-induced mouse models for PAH, which was accompanied with the activation of autophagy and phenotypic switching to a synthetic phenotype of VSMCs. Overexpression of SUMO1 promoted VSMCs proliferation, migration and dedifferentiation via activated autophagy under hypoxia. Moreover, we provide evidence that SUMO1 regulates the activation of autophagy by inducing SUMOylation of Vps34 and the formation of the Beclin-1-Vps34-Atg14L complex.

2. Methods

2.1. Plasmids, and antibodies

The construction of the PCMV-HA-SUMO1 plasmid for overexpression of SUMO1 (human SUMO1 cDNA, sequence ID: NM_003352.4) was prepared by RT-PCR analysis using HEK293 RNA samples and subcloning into the PCMV-HA vector digested with Bgl II and Not I. The construction of the PCMV-Myc-WT-Vps34 plasmid for overexpression of Vps34 (human Vps34 cDNA, sequence ID: NM_002647.3) was prepared by RT-PCR analysis using Hela RNA samples and subcloning into the PCMV-Myc vector digested with EcoR I and Xho I. The PCMV-Myc-WT-Vps34 plasmid was mutated into PCMV-Myc-M840-VPS34 containing a K840R mutation using PCR-based site-directed mutagenesis as previously described [45].

Antibodies against SM22, α-SMA, and SM-MHC were from Biosynthesis Biotechnology. Antibodies against SUMO1, GAPDH, p62, and LC3b were from Affinity Biosciences, Abcam, Proteintech, and Cell Signaling Technology, respectively.

2.2. Cell culture and transfection

Human pulmonary arterial SMCs (PASMCS, ATCC) were cultured in the vascular cell basal medium (ATCC PCS-100-030) supplemented with the vascular smooth muscle growth kit (ATCC PCS-100-042) according to the manufacturer's instruction. The cells were cultured at

5% CO_2 and 37 °C in a humidified cell culture incubator. Either plasmid DNA (2 μg) or SUMO1 siRNA (Ribobio, Guangzhou, China) was transfected into PASMCS using Viafect according to the manufacturer's instruction (Promega, Madison, WI, USA).

MOVAS-1, a mouse aortic VSMCs line (ATCC), was cultured in Dulbecco's Modified Eagle's medium (DMEM) with 10% fetal bovine serum (FBS) (Gibco Life Technologies, Gaithersburg, MD, USA). The cells were cultured at 5% CO_2 and 37 °C in a humidified cell culture incubator. Plasmid DNA (2 μg) was transfected into MOVAS-1 using Viafect according to the Manufacturer's instruction (Promega, Madison, WI, USA).

For hypoxia treatment, cell culture was incubated in a Hypoxia Chamber (HF100 Incubator, Heal Force Bio-Meditech Holdings Limited, Shanghai, PRC) with 3% O2, 5% CO2, and 92% N2. Cells were cultured in 6-well plates and exposed to hypoxia for 24 h.

2.3. Animals

We utilized C57BL/6 male mice (8–12 weeks) in all animal experiments. This study was approved by the Ethics Committee on Animal Research of Huazhong University of Science and Technology.

2.4. Mouse models for PAH

Two mouse models for PAH were established as described previously [46,47]. For the hypoxia-induced PAH model, C57BL/6 mice were randomly divided into two groups. The control group was exposed to a normoxic condition (normal oxygen). The experimental group was exposed to a hypoxic condition with 10% oxygen using a 500-liter ventilation chamber for 4 weeks [48]. For the MCT-induced PAH model, C57BL/6 male mice were also randomly divided into two groups. MCT was dissolved in ethanol at a ratio of 2:8 using normal saline. The experimental group was injected subcutaneously with MCT at a dose of 600 mg/kg body weight once a week for four weeks. The control group was injected subcutaneously with the same volume of solvent. All mice were housed under a constant temperature of 22 °C and alternate cycles of 12 h of light and 12 h of darkness. All mice were fed with a standard mouse chow diet and water.

2.5. Phenotyping of PAH mice

The mean value of pulmonary arterial pressure (mPAP) was measured in PAH mice and control mice by inserting a 1.4F Millar Mikro-tip catheter-transducer through the right jugular vein and into the pulmonary artery as previously described [49]. The right ventricle (RV) and left ventricle plus septum (LV + Septum) were excised from the heart and weighed as previously described [3]. The ratio of RV/(LV + Septum) was used as an indicator of right ventricle (RV) hypertrophy.

The percentage of wall thickness of the media was measured as previously described [49,50]. The percentage of vascular media wall thickness was calculated by the formula: vascular media wall thickness (%) = area ext − area int/area ext × 100.

For measurement of muscularization, lung sections (5 μm) were stained for smooth muscle actin (α-SMA) to investigate the degree of muscle formation in lung tissues. These arteries

were scored according to the degree whether they were completely muscular as previously described [51].

The cardiac output was measured using the Vevo-2100 Ultrasound system as described previously [52].

2.6. Cell proliferation assays

PASMCs and MOVAS-1 were seeded into 96-well plates at a density of 5×10^3 per well. After 24 h of culture, cells were transfected with a SUMO1 expression plasmid or SUMO1 siRNA for 36 h. The transfected cells were used for cell proliferation assays with the 2-(2-methoxy-4-nitrophenyl)-3-(4-nitrophenyl)-5-(2,4-disulfophenyl)-2H-tetrazolium, monosodium salt (WST-8) kit (Cell Counting Kit-8 or CCK-8, Dojindo Laboratories) [7,35]. In brief, 10 μl of the CCK-8 solution was added to the cell culture and incubated for 2 h. We then measured the rate of cell proliferation by reading absorbance at 450 nm with a microplate reader.

2.7. Number of cells at the S phase during cell cycle

Cell cycle analysis was performed with PASMCs and MOVAS-1 cells transfected with a SUMO1 expression plasmid or SUMO1 siRNA as described [7]. The transfection was carried out at a cell density of 5×10^5 in six-well plates for 36 h. The transfected cells were washed with PBS, digested with tyrisin, immobilized with ethanol, and stained with propidium iodide (PI) for 30 min. Beckman Coulter Cytomics FC 500 flow cytometry and CXP software (Beckman Coulter) were used for cell cycle analysis.

2.8. Cell migration

For cell migration, PASMCs and MOVAS-1 cells were seeded into six-well plates at a density of 5×10^5 in six-well plates, and cultured under standard conditions for 24 h. Cells were then transfected with a SUMO1 expression plasmid or SUMO1 siRNA for 36 h. Monolayer cells were scraped off with a 200 μl pipette tip to make a scratch wound. Cell migration was determined by measuring the distance of movement of cells into the scraped area after 12 h. The scratches were visualized with a microscope and photographed.

2.9. Real-time qRT-PCR analysis

Total RNA samples were extracted from transfected cells or mouse tissue samples using Trizol (Invitrogen) according to the manufacturer's instruction. A total of 0.5 μg of RNA samples were converted to cDNA using M-MLV reverse transcriptase according to the manufacturer's protocol (Promega, Madison, WI, USA), and used for real-time RT-PCR analysis. Quantitative real-time PCR analysis was performed using a FastStart Universal SYBR Green Master (Roche, Basel, BS, Switzerland) and 7900 HT Fast Real-Time PCR System (Thermo, Waltham, MA, USA) as previously described [35,53]. Experiments were performed in triplicate and repeated at least three times.

2.10. Western blot analysis

Western blot analysis was carried out using lung samples or cultured and transfected PASMCs or MOVAS-1 with different antibodies as described previously [53-55]. Mice were

anesthetized with an intraperitoneal injection of sodium pentobarbital (50 mg/kg body weight), and lungs were dissected out for extraction of total protein extracts. Transfected PASMCs or MOVAS-1 cells were washed three times with PBS and then used for extraction of total protein extracts by lysis in 20 mM Tris-HCl, pH 7.6, 150 mM NaCl, 0.1% DOC, 0.5% NP-40, 10% glycerol, 1 mM glycerophosphate, 1 mM NaF, 2.5 mM Na pyrophosphate, 1 mM Na3VO4, and a cocktail of protease inhibitors (Calbiochem, Millipore, MA, USA) at 4 °C. Protein extracts were then mixed with reducing loading buffer, boiled for 15 min, centrifuged for 10 min, separated by SDS-PAGE, and transferred to nitrocellulose membranes. The nitrocellulose membranes were cut into different slices according to the sizes of the target proteins and the control GAPDH, and then used for Western blot analysis. We used the 1-D analysis software and Quantity One (Bio-Rad, Hercules, CA, USA) to capture Western blot images and quantify the intensity of protein band signals [45,53,54]. Each experiment was repeated at least three times.

2.11. Co-IP (co-immunoprecipitation) assay

Total protein extracts from transfected MOVAS-1 cells were extracted with ice-cold lysis buffer containing 25 mM Tris-HCl (pH 8.0), 150 mM NaCl, 0.5% NP-40, 1% SDS, 200 μM sodium deoxycholate, 1 mM dithiothreitol, 5 mM EDTA, 0.5 mM phenylmethanesulfonyl-fluoride, 10 mM N-ethylmaleimide (NEM-23030), 10 mM iodoacetamide and a cocktail of protease inhibitors. The lysates were then subjected to immunoprecipitation and Western blotting as described previously [35].

2.12. Statistical analysis

We designed experiments and perfume statistical analyses as previously recommended [56]. All quantitative data were shown as mean ± standard deviation (S.D.). The differences between two groups of variables were compared by the two-tailed, paired or unpaired Student's t-test. For comparisons of more than two groups, one-way analysis of variance was employed for normal distributions and the Kruskal-Wallis test for non-normal or small samples. A P value of < 0.05 was considered as significant.

3. Results

3.1. Association of increased SUMO1 expression with the activation of autophagy in a hypoxia-induced PAH model

In order to study the molecular pathogenic mechanism of PAH, we established a mouse model for PAH. We exposed mice to a continuous hypoxic condition for 4 weeks, which resulted in PAH. Compared to control mice exposed to a normoxic condition, the mice under hypoxia developed PAH with a significant increase of mPAP (Fig. 1A), RV/(LV + Septum) (Fig. 1B) or total pulmonary resistance (Fig. 1C). Compared with control mice, the cardiac output of PAH mice was not changed (Fig. 1D). The thickness of the arterial wall of small pulmonary arteries was significantly increased in hypoxic PAH mice as compared with control mice (Fig. 1E and F).

Western blot analysis with lung tissue samples showed that the expression level of SUMO1 was significantly increased in hypoxic PAH mice compared to control mice (Fig. 2A and B).

Interestingly, the level of autophagy activation (increased LC3b expression levels and decreased p62 expression levels) was significantly increased in hypoxic PAH mice compared to control mice (Fig. 2A and B). These studies revealed an association between increased SUMO1 expression and induction of autophagy in a hypoxic PAH mouse model.

3.2. VSMCs phenotypic switching in hypoxic PAH mice

We analyzed the expression levels of contractile VSMCs markers αSMA, SM22 and SM-MHC to determine whether there is phenotypic switching of VSMCs to a synthetic phenotype (dedifferentiation) in hypoxic PAH mice. Real-time RT-PCR analysis showed that the expression levels of VSMCs contractile marker genes encoding αSMA, SM22 and SM-MHC were significantly reduced in hypoxic PAH mice compared with that in control mice (Fig. 3A). These results were confirmed at the protein level using Western blot analysis (Fig. 3B and C).

3.3. Increased SUMO1 expression, induction of autophagy and phenotypic switching in a MCT-induced PAH model

To further study the molecular pathogenic mechanism of PAH, we established another mouse model for PAH, the MCT-induced model for PAH. The thickness of the wall of small pulmonary arteries was significantly increased in MCT PAH mice as compared with control mice (Fig. 4A and B). Western blot analysis with lung tissue samples showed that the expression level of SUMO1 was significantly increased in MCT PAH mice compared to control mice (Fig. 4C and D). Interestingly, the level of autophagy activation (increased LC3b expression levels and decreased p62 expression levels) was also significantly increased in MCT PAH mice as compared to control mice (Fig. 4C and D). We also analyzed the expression levels of contractile VSMC markers α–SMA, SM22 and SM-MHC to determine whether there is phenotypic switching of VSMCs to a synthetic phenotype (dedifferentiation) in MCT PAH mice. The expression levels of α–SMA, SM22 and SM-MHC were significantly reduced in MCT PAH mice compared with that in control mice (Fig. 4E and F).

3.4. SUMO1 accelerates hypoxia-induced proliferation and migration of VSMCs

MOVAS-1 were transfected with a mammalian expression plasmid for SUMO1 or control empty vector, exposed to hypoxia for 48 h, and used for cell proliferation and migration analyses as well as cell cycle analysis. Cell proliferation assays with the CCK-8 kit showed that hypoxia induced VSMCs proliferation, and overexpression of SUMO1 further increased VSMCs proliferation (Fig. 5A). Similar findings were made for the expression level of cell proliferation marker Ki-67 (Fig. 5B). Cell cycle analysis using flow cytometry showed that hypoxia significantly increased the number of cells at the S phase during cell division, and overexpression of SUMO1 further increased the number of cells at the S phase (Fig. 5C). Cell migration analysis using the scratch-wound healing assay showed that hypoxia stimulated migration of VSMCs, and overexpression of SUMO1 further accelerated the migration of VSMCs (Fig. 5D). Cell apoptosis using flow cytometry showed that hypoxia significantly decreased the number of apoptotic cells, and SUMO1 overexpression further reduced the apoptosis of VSMCs (Fig. 5E and F).

3.5. SUMO1 regulates hypoxia-induced VSMCs phenotypic switching by activating autophagy

In order to further determine the role of SUMO1 in hypoxia-induced VSMC phenotypic switching, we characterized the effect of SUMO1 overexpression and autophagy inhibitor 3-MA on the expression levels of α-SMA, SM22 and SM-MHC (Fig. 6A). Western blot analysis showed that hypoxia significantly reduced the expression levels of α-SMA, SM22 and SM-MHC, which was further reduced by SUMO1 overexpression (Fig. 6A). Meanwhile, Western blot analysis showed that SUMO1 overexpression significantly increased the level of autophagy induced by hypoxia (increased levels of LC3b and decreased levels of p62) (Fig. 6A). To determine whether the effect of SUMO1 overexpression on VSMC phenotypic switching is due to activation of autophagy, we treated MOVAS-1 cells with a pharmacological inhibitor of autophagy, 3-methyladenine (3-MA), prior to hypoxia. As shown in (Fig. 6B), the inhibition of autophagy decreased the effect of SUMO1 overexpression on the expression levels of αSMA, SM22 and SM-MHC. Autophagy inhibitor 3-MA also diminished the effect of increased VSMC proliferation induced by SUMO1 overexpression (Fig. 6C).

3.6. SUMO1 knockdown reversed hypoxia-induced proliferation and migration of PASMCs

Human PASMCs were transfected with SUMO1-speccific siRNA or control siNC, exposed to hypoxia for 48 h, and used for cell proliferation, migration, cell cycle and apoptosis analyses. Cell proliferation assays with the CCK-8 kit showed that hypoxia induced significantly increased proliferation of PASMCs, however, the effect was inhibited by SUMO1 knockdown (Fig. 7A). Similar findings were made for the expression level of cell proliferation marker Ki-67 (Fig. 7B). Cell cycle analysis using flow cytometry showed that hypoxia significantly increased the number of cells at the S phase during cell division, however, the effect was inhibited by SUMO1 knockdown (Fig. 7C). Cell migration analysis using the scratch-wound healing assay showed that hypoxia stimulated the migration of PASMCs, however, the effect was inhibited by SUMO1 knockdown (Fig. 7D). Cell apoptosis analysis using flow cytometry showed hypoxia significantly decreased apoptosis, however, the effect was inhibited by SUMO1 knockdown (Fig. 7E and F). In addition, we determined the role of SUMO1 in hypoxia-induced phenotypic switching and autophagy activation of PASMCs. Western blot analysis showed that hypoxia significantly reduced the expression levels of α-SMA, SM22 and SM-MHC, and the effect was attenuated by SUMO1 knockdown (Fig. 7G and H). Meanwhile, Western blot analysis showed that SUMO1 knockdown significantly decreased the level of autophagy induced by hypoxia (increased levels of LC3b and decreased levels of p62) (Fig. 7G and H).

3.7. SUMO1 binds to and SUMOylates Vps34, increases the autophagy initiation complex formation among Beclin-1, Vps34 and ATG14L, and promotes hypoxia-induced VSMCs phenotypic switching

SUMOylation of phosphatidylinositol 3-kinase Vps34 was shown to induce autophagy [57]. We, therefore, determined whether SUMO1 causes Vps34 SUMOylation, and whether this induces autophagy and VSMC phenotypic switching under hypoxia. Myc-tagged Vps34 was co-transfected with FLAG-tagged SUMO-1 into MOVAS-1 cells, which were treated with or

without hypoxia. Western blot analysis showed that hypoxia induced the binding of SUMO1 to endogenous Vps34 with in VSMCs (Fig. 8A and B).

We previously showed that the formation of the Beclin-1-Vps 34-Atg14L complex is involved in autophagy activation [35]. Because SUMO1 increased hypoxia-induced autophagy, we analyzed the effect of SUMO1 on the assembly of the Beclin-1-Vps34-Atg14L complex. Co-immunoprecipitation assays showed that hypoxia increased the complex formation between Beclin-1 and Vps34 and between Beclin-1and Atg14L (Fig. 8C and D), and overexpression of SUMO1 further increased the complex formation among Beclin-1, Vps34, and Atg14L (Fig. 8C and D).

To determine the effect of Vps34 SUMOylation on hypoxia-induced VSMC phenotypic switching, we characterized a mutation in Vps34, which substitutes the K residue at codon 840 with an R residue (K840R), a mutation that prevents SUMOylation of Vps34 at K840 [57]. Co-immunoprecipitation assays showed that SUMOylation of Vps34 was significantly decreased in MOVAS-1 cells by mutation K840R (Fig. 8E and F). Western blot analysis also showed that compared with wild type (WT) Vps34, mutant Vps34 with the K840R mutation had significantly increased levels of αSMA, SM22 and SM-MHC in hypoxia (Fig. 8G and H), which suggests that mutation K840R blocks the Vps34-induced VSMC phenotypic switching to a synthetic phenotype.

Together, our data support a working model in which hypoxia increases the expression level of SUMO1, which leads to Vps34 SUMOylation, resulting in increased complex formation among Beclin-1, Vps34, and Atg14L; The Becn-1-Vps 34-Atg14L complex induces autophagy activation, which leads to hypoxia-induced VSMCs phenotypic switching to a synthetic phenotype (dedifferentiation), and increased VSMC proliferation and migration, resulting in pulmonary vascular remolding, and PAH (Fig. 9).

4. Discussion

In this study, we identified a novel molecular pathway critical to pulmonary vascular remodeling and PAH. The novel pathway contains SUMO1, SUMOylation of Vps34, the formation of the Beclin-1-Vps34-Atg14L complex, and activation of autophagy (Fig. 9). The results support the key role of the SUMo1-Vps34 SUMOylation-autophagy pathway in pulmonary vascular remodeling and PAH, and suggest that the pathway may represent a potential therapeutic target for development of treatment strategies for hypoxic PAH.

SUMOylation is an important post-translational modification mechanism which plays a role in many biological functions, including cell proliferation, migration, cell stress response and tumorigenesis [58]. SUMOylation is also involved in regulation of protein subcellular localization, protein-DNA interaction, protein-protein interaction, transcriptional regulation, DNA damage repair, and genome organization [58,59]. Moreover, abnormal SUMOylation was associated with many diseases, including cardiac diseases, neurodegenerative diseases and cancers [58,60,61]. However, the role of SUMOylation was less well-studied in PAH. To date, there was one report showing that SUMO1 expression was significantly increased in the pulmonary arteries of rats under hypoxia [12]. Jiang et al. further showed that SUMO1

interacted with HIF1α, and regulated the expression levels of HIF1α and VEGFA mRNA and proteins [12]. However, the molecular pathogenic mechanism of increased SUMO1 expression in PAH is unknown. It is also unknown whether the regulation of HIF1α and VEGFA by SUMO1 is associated with pulmonary vascular remodeling and PAH. Our study here demonstrates the increased SUMO1 expression level in PAH using two mouse models, a hypoxia-induced model and another MCT-induced model. Most importantly, we uncovered a novel molecular mechanism by which SUMO1 overexpression causes hypoxia-induced VSMCs proliferation, migration, autophagy activation, and dedifferentiation, pulmonary vascular remodeling and PAH (Fig. 9). Therefore, our data provide important insights into the molecular pathogenic mechanisms of PAH.

A prominent feature of PAH is the increased proliferation and reduced apoptosis of PASMCs [44]. In this study, we found that SUMO1 overexpression increased VSMC proliferation, and SUMO1-induced autophagy activation is required for the process (Fig. 6). SUMO1 promoted a robust activation of autophagy characterized by increased LC3b levels and decreased p62 levels in VSMCs, and inhibition of autophagy by 3-MA prevented VSMCs proliferation induced by SUMO1 overexpression (Fig. 6). This is consistent with a recent finding showing that 3-MA prevented arterial restenosis [62]. The role of autophagy in PAH is interesting. One study showed that the expression level of LC3b was significantly increased in lung tissue samples from PAH patients compared with normal control patients [63]. Another study showed that LC3b expression was increased and p62 expression was reduced in lung samples from MCT-induced PAH rats [44]. These data indicate that autophagy was significantly activated in PAH. On the other hands, knockout animal studies revealed conflicting results about the role of autophagy in PAH. *LC3b*$^{-/-}$ knockout mice were more susceptibility to hypoxia-induced PAH [48], but autophagy deficiency *Becn1*$^{+/-}$ mice did not demonstrate an accelerated pulmonary hypertensive response to hypoxia [48]. Our data in this study support a role of autophagy in the pathogenesis of PAH. Most importantly, here we identified a novel mechanism involving SUMO1 overexpression and SUMO1-mediated SUMOylation of Vps34 for activation of autophagy involved in VSMCs functions and pulmonary vascular remodeling.

Despite the novel findings from the present study, there are several issues that remain to be addressed in the future. First, in addition to VSMCs, SUMO1 is also expressed in endothelial cells, which are important for the pathogenesis of PAH. Future studies with pulmonary endothelial cells may determine whether SUMO1 plays a role in endothelial functions relevant to PAH and whether SUMO1 is important for a mechanism termed endothelial-to-mesenchymal transition (EndMT) involved in PAH. Second, cell type-specific knockout of SUMO1 in animals may identify other novel endothelia cell-specific or VSMCs-specific molecular mechanisms for the pathogenesis of pulmonary vascular remodeling and PAH. Third, the molecular signaling pathway upstream of hypoxia-induced SUMO1 up-regulation remains to be fully identified. Fourth, SUMO1 can regulate SUMOylation of numerous other proteins. In addition to Vps34, some other substrates of SUMO1 may also be involved in the pathogenesis of PAH. For example, SUMO1 can regulate p53 SUMOylation and the stability of p53 [64,65].

Future studies can investigate whether SUMO1-induced p53 SUMOylation plays any role in the pathogenesis of PAH. In addition, SUMO1 plays an important role in DNA damage responses [66], and the DNA damage and ROS levels in pulmonary artery endothelial cells were much higher in PAH patients than in non-PAH controls [67,68]. SUMO1 has many substrates involved in DNA damage and repair, including Rad1 that binds to DNA lesion sites through SUMOylation [69], PCNA, TLS polymerase polη and REV1, XPC, Yku70, TDG, UL44, FANCI, FANCD2, Rad52, Sae2, Mre11-Rad50-Xrs2 (MRX), Lif1, PICH, PARP1, MDC1, and others [70]. Hence, it may be interesting to determine whether SUMO1 also regulates PAH development by regulating SUMOylation of proteins involved in DNA damage responses.

5. Conclusions

In summary, we have demonstrated that SUMO1 plays a critical role in PAH as a modulator of hypoxia-induced VSMCs proliferation, migration, autophagy activation, and dedifferentiation, and pulmonary arterial remodeling. We also uncovered a novel molecular mechanism underlying these processes, which involves SUMO1-induced SUMOylation of Vps34, the formation of the Beclin-1-Vps34-Atg14L complex, and the activation of autophagy. Inhibition of SUMO1-induced autophagy may mitigate pulmonary arterial VSMCs proliferation and hypoxia-induced pulmonary arterial remodeling. This may serve as a potential target for the treatment of PAH.

Acknowledgements

We thank other members of the Center for Human Genome Research for help and assistance.

Sources of funding

This study was supported by the National Natural Science Foundation of China grants (81630002, 31430047 and 91439129), the Hubei Province Natural Science Program Innovative Team grant (2017CFA014), China Postdoctoral Science Foundation funded project (2017M622409) and Certificate of China Postdoctoral Science Foundation fund (2018T110754).

Abbreviations:

SUMO1	small ubiquitin-related modifier 1
PAH	Pulmonary arterial hypertension
VSMCs	vascular smooth muscle cells

References

[1]. Stenmark KR, Fagan KA, Frid MG, Hypoxia-induced pulmonary vascular remodeling: cellular and molecular mechanisms, Circ. Res 99 (2006) 675–691. [PubMed: 17008597]

[2]. Guignabert C, Dorfmuller P, Pathology and pathobiology of pulmonary hypertension, Semin. Respir. Crit. Care Med 38 (2017) 571–584. [PubMed: 29032561]

[3]. Zhang W, Zhu T, Wu W, Ge X, Xiong X, Zhang Z, et al., LOX-1 mediated phenotypic switching of pulmonary arterial smooth muscle cells contributes to hypoxic pulmonary hypertension, Eur. J. Pharmacol 818 (2017) 84–95. [PubMed: 29069578]

[4]. Zhu B, Gong Y, Yan G, Wang D, Qiao Y, Wang Q, et al., Down-regulation of lncRNA MEG3 promotes hypoxia-induced human pulmonary artery smooth muscle cell proliferation and migration via repressing PTEN by sponging miR-21, Biochem. Biophys. Res. Commun (2017) 2125–2132. [PubMed: 29198701]

[5]. Yi B, Cui J, Ning JN, Wang GS, Qian GS, Lu KZ, Over-expression of PKGIalpha inhibits hypoxia-induced proliferation, Akt activation, and phenotype modulation of human PASMCs: the role of phenotype modulation of PASMCs in pulmonary vascular remodeling, Gene 492 (2012) 354–360. [PubMed: 22101188]

[6]. Owens GK, Regulation of differentiation of vascular smooth muscle cells, Physiol. Rev 75 (1995) 487–517. [PubMed: 7624392]

[7]. Yao Y, Hu Z, Ye J, Hu C, Song Q, Da X, et al., Targeting AGGF1 (angiogenic factor with G patch and FHA domains 1) for blocking neointimal formation after vascular injury, J. Am. Heart. Assoc 6 (2017).

[8]. Schultz K, Fanburg BL, Beasley D, Hypoxia and hypoxia-inducible factor-1alpha promote growth factor-induced proliferation of human vascular smooth muscle cells, Am. J. Physiol. Heart Circ. Physiol 290 (2006) H2528–H2534. [PubMed: 16399861]

[9]. Iwata K, Ikami K, Matsuno K, Yamashita T, Shiba D, Ibi M, et al., Deficiency of NOX1/nicotinamide adenine dinucleotide phosphate, reduced form oxidase leads to pulmonary vascular remodeling, Arterioscler. Thromb. Vasc. Biol 34 (2014) 110–119. [PubMed: 24233492]

[10]. Erzurum S, Rounds SI, Stevens T, Aldred M, Aliotta J, Archer SL, et al., Strategic plan for lung vascular research: an NHLBI-ORDR Workshop Report, Am. J. Respir. Crit. Care Med 182 (2010) 1554–1562. [PubMed: 20833821]

[11]. Grillari J, Grillari-Voglauer R, Jansen-Durr P, Post-translational modification of cellular proteins by ubiquitin and ubiquitin-like molecules: role in cellular senescence and aging, Adv. Exp. Med. Biol 694 (2010) 172–196. [PubMed: 20886764]

[12]. Jiang Y, Wang J, Tian H, Li G, Zhu H, Liu L, et al., Increased SUMO-1 expression in response to hypoxia: interaction with HIF-1alpha in hypoxic pulmonary hypertension, Int. J. Mol. Med 36 (2015) 271–281. [PubMed: 25976847]

[13]. Hochstrasser M, SP-RING for SUMO: new functions bloom for a ubiquitin-like protein, Cell 107 (2001) 5–8. [PubMed: 11595179]

[14]. Su HL, Li SS, Molecular features of human ubiquitin-like SUMO genes and their encoded proteins, Gene 296 (2002) 65–73. [PubMed: 12383504]

[15]. Saitoh H, Pu RT, Dasso M, SUMO-1: wrestling with a new ubiquitin-related modifier, Trends Biochem. Sci 22 (1997) 374–376. [PubMed: 9357311]

[16]. Shao R, Zhang FP, Rung E, Palvimo JJ, Huhtaniemi I, Billig H, Inhibition of small ubiquitin-related modifier-1 expression by luteinizing hormone receptor stimulation is linked to induction of progesterone receptor during ovulation in mouse granulosa cells, Endocrinology 145 (2004) 384–392. [PubMed: 14500579]

[17]. Shao R, Zhang FP, Tian F, Anders Friberg P, Wang X, Sjoland H, et al., Increase of SUMO-1 expression in response to hypoxia: direct interaction with HIF-1alpha in adult mouse brain and heart in vivo, FEBS Lett. 569 (2004) 293–300. [PubMed: 15225651]

[18]. Archer SL, Mitochondrial dynamics–mitochondrial fission and fusion in human diseases, N. Engl. J. Med 369 (2013) 2236–2251. [PubMed: 24304053]

[19]. Chan DC, Fusion and fission: interlinked processes critical for mitochondrial health, Annu. Rev. Genet 46 (2012) 265–287. [PubMed: 22934639]

[20]. Atkins K, Dasgupta A, Chen KH, Mewburn J, Archer SL, The role of Drp1 adaptor proteins MiD49 and MiD51 in mitochondrial fission: implications for human disease, Clin. Sci 130 (2016) 1861–1874. [PubMed: 27660309]

[21]. Wauchope OR, Mitchener MM, Beavers WN, Galligan JJ, Camarillo JM, Sanders WD, et al., Oxidative stress increases M1dG, a major peroxidation-derived DNA adduct, in mitochondrial DNA, Nucleic Acids Res. 46 (2018) 3458–3467. [PubMed: 29438559]

[22]. Boucherat O, Peterlini T, Bourgeois A, Nadeau V, Breuils-Bonnet S, Boilet-Molez S, et al., Mitochondrial HSP90 accumulation promotes vascular remodeling in pulmonary arterial hypertension, Am. J. Respir. Crit. Care Med 198 (2018) 90–103. [PubMed: 29394093]

[23]. Zunino R, Schauss A, Rippstein P, Andrade-Navarro M, McBride HM, The SUMO protease SENP5 is required to maintain mitochondrial morphology and function, J. Cell Sci 120 (2007) 1178–1188. [PubMed: 17341580]

[24]. Harder Z, Zunino R, McBride H, Sumo1 conjugates mitochondrial substrates and participates in mitochondrial fission, Curr. Biol.: CB 14 (2004) 340–345. [PubMed: 14972687]

[25]. Santel A, Fuller MT, Control of mitochondrial morphology by a human mitofusin, J. Cell Sci 114 (2001) 867–874. [PubMed: 11181170]

[26]. Chen KH, Dasgupta A, Lin J, Potus F, Bonnet S, Iremonger J, et al., Epigenetic dysregulation of the dynamin-related protein 1 binding partners MiD49 and MiD51 increases mitotic mitochondrial fission and promotes pulmonary arterial hypertension: mechanistic and therapeutic implications, Circulation 138 (2018) 287–304. [PubMed: 29431643]

[27]. Gill G, SUMO and ubiquitin in the nucleus: different functions, similar mechanisms? Genes Dev. 18 (2004) 2046–2059. [PubMed: 15342487]

[28]. Hilgarth RS, Murphy LA, Skaggs HS, Wilkerson DC, Xing H, Sarge KD, Regulation and function of SUMO modification, J. Biol. Chem 279 (2004) 53899–53902. [PubMed: 15448161]

[29]. Hu J, Xue P, Mao X, Xie L, Li G, You Z, SUMO1/UBC9decreased Nox1 activity inhibits reactive oxygen species generation and apoptosis in diabetic retinopathy, Mol. Med. Rep 17 (2018) 1690–1698. [PubMed: 29138839]

[30]. Brun S, Abella N, Berciano MT, Tapia O, Jaumot M, Freire R, et al., SUMO regulates p21Cip1 intracellular distribution and with p21Cip1 facilitates multi-protein complex formation in the nucleolus upon DNA damage, PLoS One 12 (2017) e0178925. [PubMed: 28582471]

[31]. Hou X, Yang Z, Zhang K, Fang D, Sun F, SUMOylation represses the transcriptional activity of the Unfolded Protein Response transducer ATF6, Biochem. Biophys. Res. Commun 494 (2017) 446–451. [PubMed: 29061306]

[32]. Tang JL, Zhang HH, Lai MD, Role of autophagy and apoptosis in tumor, Zhonghua bing li xue za zhi = Chin. J. Pathol 41 (2012) 573–576.

[33]. Klionsky DJ, Emr SD, Autophagy as a regulated pathway of cellular degradation, Science 290 (2000) 1717–1721. [PubMed: 11099404]

[34]. Levine B, Kroemer G, Autophagy in the pathogenesis of disease, Cell 132 (2008) 27–42. [PubMed: 18191218]

[35]. Lu Q, Yao Y, Hu Z, Hu C, Song Q, Ye J, et al., Angiogenic factor AGGF1 activates autophagy with an essential role in therapeutic angiogenesis for heart disease, PLoS Biol. 14 (2016) e1002529. [PubMed: 27513923]

[36]. Mizushima N, Autophagy: process and function, Genes Dev. 21 (2007) 2861–2873. [PubMed: 18006683]

[37]. Jones SA, Mills KH, Harris J, Autophagy and inflammatory diseases, Immunol. Cell Biol 91 (2013) 250–258. [PubMed: 23318657]

[38]. Ryter SW, Cloonan SM, Choi AM, Autophagy: a critical regulator of cellular metabolism and homeostasis, Mol. Cell 36 (2013) 7–16.

[39]. Ryter SW, Lee SJ, Choi AM, Autophagy in cigarette smoke-induced chronic obstructive pulmonary disease, Expert Rev. Respir. Med 4 (2010) 573–584. [PubMed: 20923337]

[40]. Ryter SW, Chen ZH, Kim HP, Choi AM, Autophagy in chronic obstructive pulmonary disease: homeostatic or pathogenic mechanism? Autophagy 5 (2009) 235–237. [PubMed: 19066468]

[41]. Patel AS, Lin L, Geyer A, Haspel JA, An CH, Cao J, et al., Autophagy in idiopathic pulmonary fibrosis, PLoS One 7 (2012) e41394. [PubMed: 22815997]

[42]. Araya J, Kojima J, Takasaka N, Ito S, Fujii S, Hara H, et al., Insufficient autophagy in idiopathic pulmonary fibrosis, Am. J. Physiol. Lung Cell Mol. Physiol 304 (2013) L56–L69. [PubMed: 23087019]

[43]. Kuwano K, Araya J, Hara H, Minagawa S, Takasaka N, Ito S, et al., Cellular senescence and autophagy in the pathogenesis of chronic obstructive pulmonary disease (COPD) and idiopathic pulmonary fibrosis (IPF), Respir. Investig 54 (2016) 397–406.

[44]. Long L, Yang X, Southwood M, Lu J, Marciniak SJ, Dunmore BJ, et al., Chloroquine prevents progression of experimental pulmonary hypertension via inhibition of autophagy and lysosomal

bone morphogenetic protein type II receptor degradation, Circ. Res 112 (2013) 1159–1170. [PubMed: 23446737]

[45]. Ye J, Yao Y, Song Q, Li S, Hu Z, Yu Y, et al., Up-regulation of miR-95-3p in hepatocellular carcinoma promotes tumorigenesis by targeting p21 expression, Sci. Rep 6 (2016) 34034. [PubMed: 27698442]

[46]. Hislop A, Reid L, New findings in pulmonary arteries of rats with hypoxia-induced pulmonary hypertension, Br. J. Exp. Pathol 57 (1976) 542–554. [PubMed: 136978]

[47]. Kay JM, Harris P, Heath D, Pulmonary hypertension produced in rats by ingestion of Crotalaria spectabilis seeds, Thorax 22 (1967) 176–179. [PubMed: 6033385]

[48]. Lee SJ, Smith A, Guo L, Alastalo TP, Li M, Sawada H, et al., Autophagic protein LC3B confers resistance against hypoxia-induced pulmonary hypertension, Am. J. Respir. Crit. Care Med 183 (2011) 649–658. [PubMed: 20889906]

[49]. Paulin R, Dromparis P, Sutendra G, Gurtu V, Zervopoulos S, Bowers L, et al., Sirtuin 3 deficiency is associated with inhibited mitochondrial function and pulmonary arterial hypertension in rodents and humans, Cell Metabol. 20 (2014) 827–839.

[50]. Li XW, Hu CP, Wu WH, Zhang WF, Zou XZ, Li YJ, Inhibitory effect of calcitonin gene-related peptide on hypoxia-induced rat pulmonary artery smooth muscle cells proliferation: role of ERK1/2 and p27, Eur. J. Pharmacol 679 (2012) 117–126. [PubMed: 22306243]

[51]. Morrell NW, Morris KG, Stenmark KR, Role of angiotensin-converting enzyme and angiotensin II in development of hypoxic pulmonary hypertension, Am. J. Physiol 269 (1995) H1186–H1194. [PubMed: 7485548]

[52]. Teng B, Tilley SL, Ledent C, Mustafa SJ, In vivo assessment of coronary flow and cardiac function after bolus adenosine injection in adenosine receptor knockout mice, Physiol. Rep 4 (2016).

[53]. Huang Y, Wang C, Yao Y, Zuo X, Chen S, Xu C, et al., Molecular basis of gene-gene interaction: cyclic cross-regulation of gene expression and post-GWAS gene-gene interaction involved in atrial fibrillation, PLoS Genet. 11 (2015) e1005393. [PubMed: 26267381]

[54]. Lu Q, Yao Y, Yao Y, Liu S, Huang Y, Lu S, et al., Angiogenic factor AGGF1 promotes therapeutic angiogenesis in a mouse limb ischemia model, PLoS One 7 (2012) e46998. [PubMed: 23110058]

[55]. Yao Y, Lu Q, Hu Z, Yu Y, Chen Q, Wang QK, A non-canonical pathway regulates ER stress signaling and blocks ER stress-induced apoptosis and heart failure, Nat. Commun 8 (2017) 133. [PubMed: 28743963]

[56]. Provencher S, Archer SL, Ramirez FD, Hibbert B, Paulin R, Boucherat O, et al., Standards and methodological rigor in pulmonary arterial hypertension preclinical and translational research, Circ. Res 122 (2018) 1021–1032. [PubMed: 29599278]

[57]. Yang Y, Fiskus W, Yong B, Atadja P, Takahashi Y, Pandita TK, et al., Acetylated hsp70 and KAP1-mediated Vps34 SUMOylation is required for autophagosome creation in autophagy, Proc. Natl. Acad. Sci. U. S. A 110 (2013) 6841–6846. [PubMed: 23569248]

[58]. Yang Y, He Y, Wang X, Liang Z, He G, Zhang P, et al., Protein SUMOylation modification and its associations with disease, Open Biol. 7 (2017).

[59]. Hickey CM, Wilson NR, Hochstrasser M, Function and regulation of SUMO proteases, Nat. Rev. Mol. Cell Biol 13 (2012) 755–766. [PubMed: 23175280]

[60]. Da Silva-Ferrada E, Ribeiro-Rodrigues TM, Rodriguez MS, Girao H, Proteostasis and SUMO in the heart, Int. J. Biochem. Cell Biol 79 (2016) 443–450. [PubMed: 27662810]

[61]. Seeler JS, Dejean A, SUMO and the robustness of cancer, Nat. Rev. Canc 17 (2017) 184–197.

[62]. Chang YJ, Huang HC, Hsueh YY, Wang SW, Su FC, Chang CH, et al., Role of excessive autophagy induced by mechanical overload in vein graft neointima formation: prediction and prevention, Sci. Rep 6 (2016) 22147. [PubMed: 26915560]

[63]. Fish JE, Matouk CC, Yeboah E, Bevan SC, Khan M, Patil K, et al., Hypoxia-inducible expression of a natural cis-antisense transcript inhibits endothelial nitric-oxide synthase, J. Biol. Chem 282 (2007) 15652–15666. [PubMed: 17403686]

[64]. Liu XM, Yang FF, Yuan YF, Zhai R, Huo LJ, SUMOylation of mouse p53b by SUMO-1 promotes its pro-apoptotic function in ovarian granulosa cells, PLoS One 8 (2013) e63680. [PubMed: 23696846]

[65]. Ivanschitz L, Takahashi Y, Jollivet F, Ayrault O, Le Bras M, de The H, PML IV/ARF interaction enhances p53 SUMO-1 conjugation, activation, and senescence, Proc. Natl. Acad. Sci. U. S. A 112 (2015) 14278–14283. [PubMed: 26578773]

[66]. Jackson SP, Durocher D, Regulation of DNA damage responses by ubiquitin and SUMO, Mol. Cell 49 (2013) 795–807. [PubMed: 23416108]

[67]. Ranchoux B, Meloche J, Paulin R, Boucherat O, Provencher S, Bonnet S, DNA damage and pulmonary hypertension, Int. J. Mol. Sci 17 (2016).

[68]. Federici C, Drake KM, Rigelsky CM, McNelly LN, Meade SL, Comhair SA, et al., Increased mutagen sensitivity and DNA damage in pulmonary arterial hypertension, Am. J. Respir. Crit. Care Med 192 (2015) 219–228. [PubMed: 25918951]

[69]. Sarangi P, Bartosova Z, Altmannova V, Holland C, Chavdarova M, Lee SE, et al., Sumoylation of the Rad1 nuclease promotes DNA repair and regulates its DNA association, Nucleic Acids Res. 42 (2014) 6393–6404. [PubMed: 24753409]

[70]. Wang Z, Zhu WG, Xu X, Ubiquitin-like modifications in the DNA damage response, Mutat. Res 803–805 (2017) 56–75.

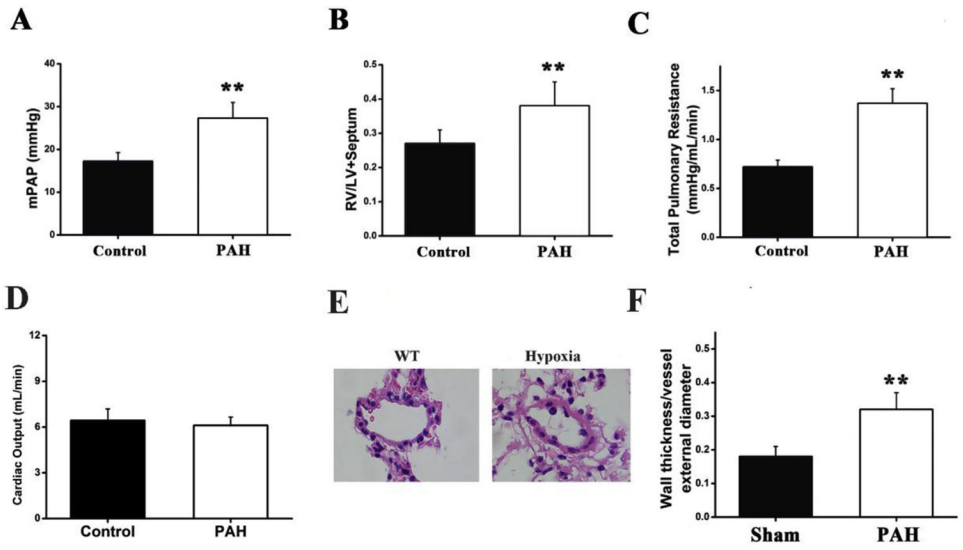

Fig. 1. Hypoxia induces pulmonary vascular remodeling and PAH in mice.

Mice were exposed to a continuous hypoxic condition for 4 weeks and characterized for the mean pulmonary artery pressure (mPAP), right ventricle/left ventricle + septum (RV/LV + S), total pulmonary resistance, and vascular remodeling in the lungs. (**A)** The mPAP was significantly increased in hypoxia-induced PAH mice compared with control mice under normoxia. (**B)** The RV/LV + S ratio was significantly increased in PAH mice compared with control mice. **(C)** The total pulmonary resistance was significantly increased in PAH mice compared with control mice. **(D)** The cardiac output was not significantly decreased in PAH mice compared with control mice. **(E)** The degree of pulmonary artery remodeling in PAH mice increased significantly compared with control mice. (**F)** Analysis of pulmonary arteries. The thickness of vessel walls was significantly increased in PAH mice compared with control mice. Fully muscularization of small pulmonary arteries was significantly increased in PAH mice compared with control mice. (n = 6/group, $*P < 0.05$, $**P < 0.01$).

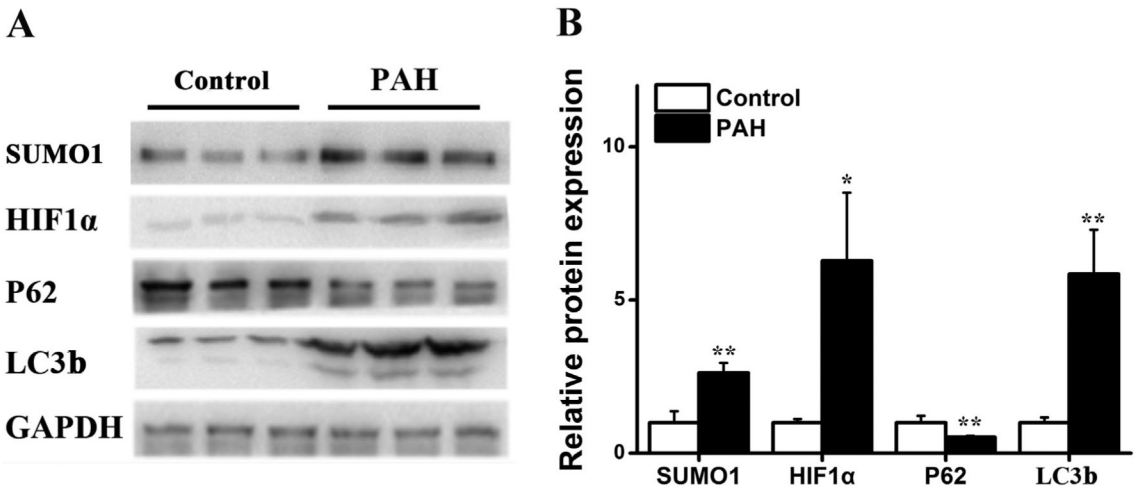

Fig. 2. Association of increased SUMO1 expression with activation of autophagy in PAH.

(A) Western blot analysis using lung tissue samples showed significantly increased expression levels of SUMO1, HIF-1α and autophagy marker LC3b, and a significantly decreased expression level of autophagy marker p62 in hypoxic PAH mice than in control mice. (**B)** The Western blotting data in (**A)** were quantified and plotted. (n = 6/group, *P < 0.05, ** $P < 0.01$).

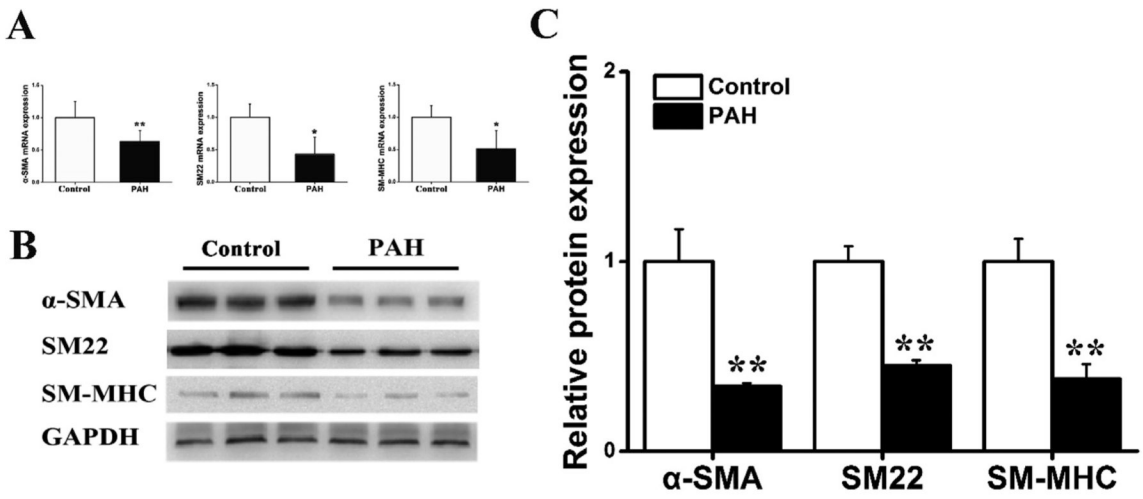

Fig. 3. VSMCs phenotypic switching in hypoxic PAH mice.

(A) Real-time RT-PCR data showed that the mRNA expression levels of contractile marker genes for α–SMA, SM22 and SM-MHC were significantly reduced in hypoxic PAH mice compared with control mice. (**B**) Western blot analysis showed that the protein expression levels of α-SMA, SM22 and SM-MHC were significantly decreased in hypoxic PAH mice compared with control mice. (**C)** Western blot data in (**B)** were quantified and plotted. (n = 6/group, *P < 0.05, ** *P* < 0.01). GAPDH was used as endogenous control.

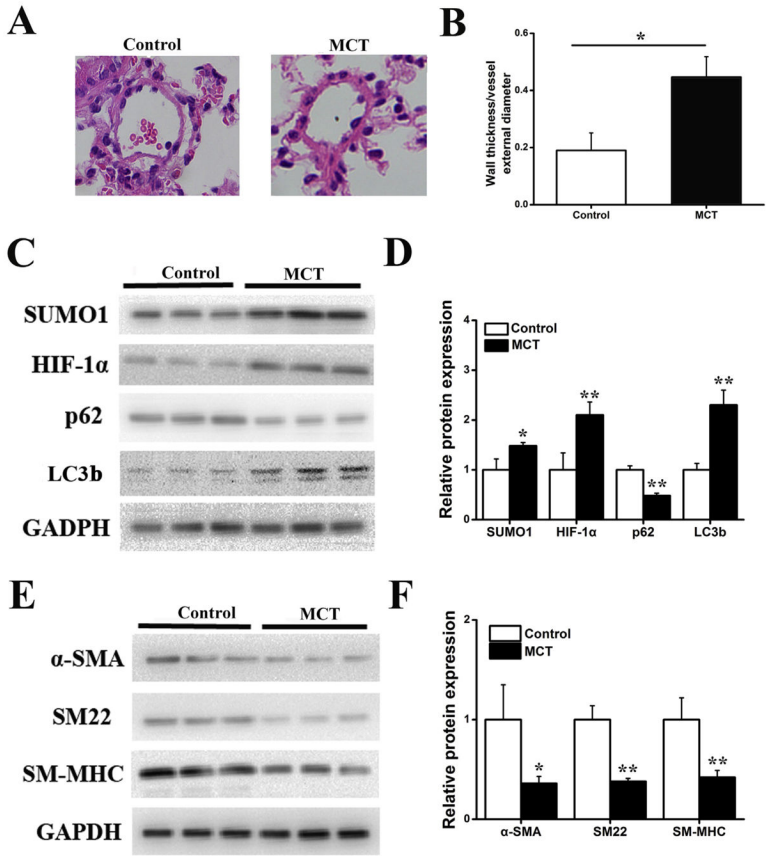

Fig. 4. Increased SUMO1 expression, induction of autophagy and phenotypic switching in a MCT-induced mouse model for PAH.

(A) The degree of pulmonary artery remodeling in MCT-treated mice increased significantly compared with control mice. (B) Analysis of pulmonary arteries. (C) Western blot analysis using lung tissue samples showing significantly increased expression levels of SUMO1, HIF-1α and autophagy marker LC3b, and a significantly decreased expression level of autophagy marker p62 in MCT-treated mice than in control mice. (**D)** Western blot data in (**C)** were quantified and plotted. (**E**) Western blot analysis showing that the protein expression levels of α-SMA, SM22 and SM-MHC were significantly decreased in hypoxic PAH mice compared with control mice. (**F)** Western blot data in (**E)** were quantified and plotted. (n = 6/group, *P < 0.05, ** *P* < 0.01).

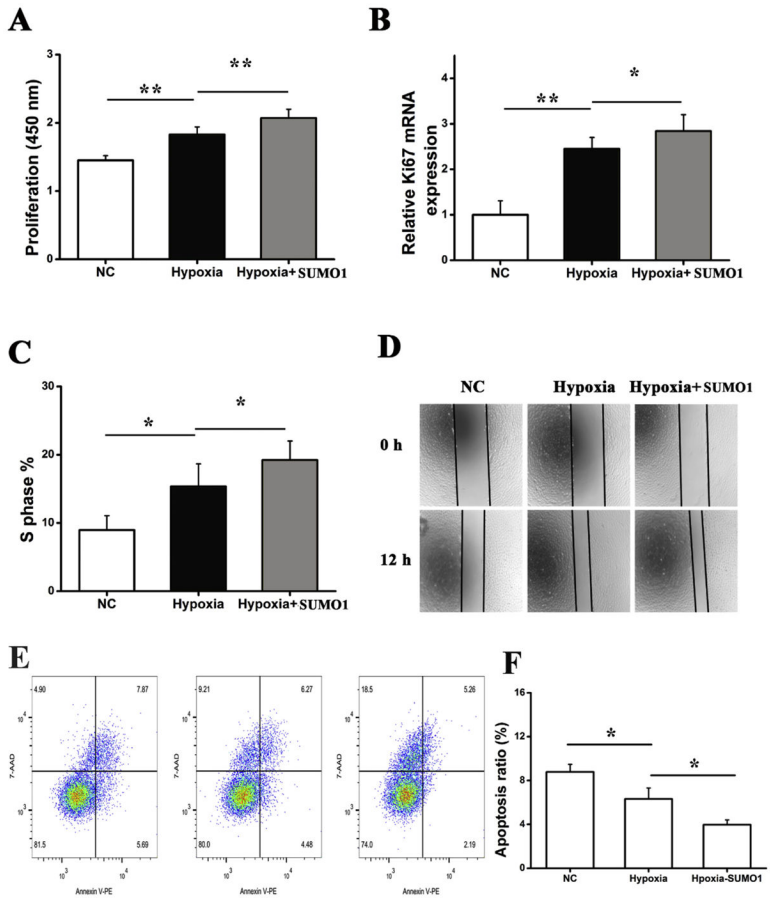

Fig. 5. Overexpression of SUMO1 increased hypoxia-induced proliferation and migration of VSMCs.

(A) Analysis of cell proliferation of the VSMCs with the CCK-8 kit by reading the optical absorbance density at 450 nm. Hypoxia increased VSMCs proliferation. Overexpression of SUMO1 further increased VSMC proliferation. (**B**) Overexpression of SUMO1 increased the hypoxia-induced increase of the mRNA expression level of Ki67 (proliferation marker). (**C**) Flow cytometry analysis to measure the number of cells at the S phase during cell division. Hypoxia significantly increased the cell number at the S phase. Overexpression of SUMO1 further increased the number of S phase cells. (**D**) Scratch-wound healing cell migration assay. Hypoxia increased the migration of VSMCs, and overexpression of SUMO1 further accelerated VSMCs migration. (E) Flow cytometry analysis to measure the number of apoptotic cells. Hypoxia significantly decreased the number of apoptotic cells. Overexpression of SUMO1 further decreased the level of apoptosis. (F) Analysis of the level of apoptosis (n = 3/group, $*P < 0.05$, $**P < 0.01$).

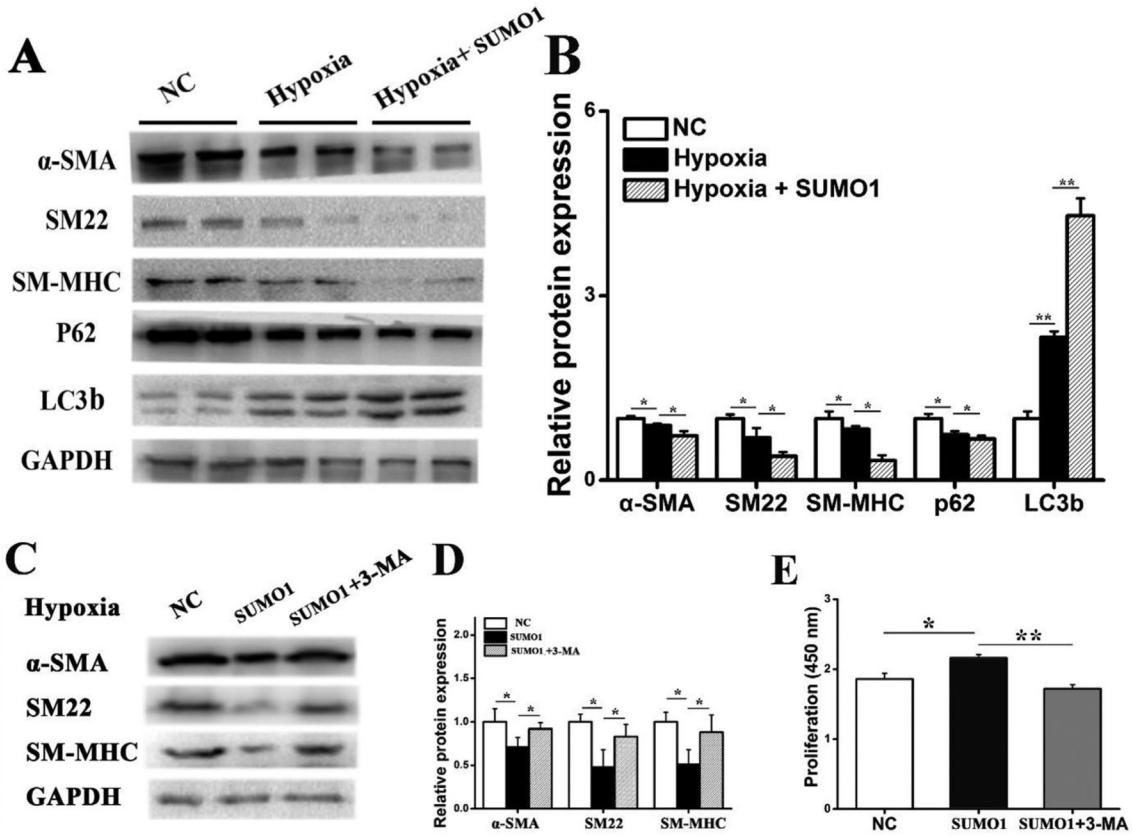

Fig. 6. SUMO1 regulates hypoxia-induced VSMCs phenotypic switching by activating autophagy.

(A) Overexpression of SUMO1 increased hypoxia-induced autophagy while decreased the expression levels of VSMCs contractile markers. Western blot analysis showed that hypoxia significantly decreased the expression levels of α–SMA, SM22 and SM-MHC. The effect was further enhanced by overexpression of SUMO1. SUMO1 significantly increased the expression level of LC3b and decreased the expression level of p62 induced by hypoxia. (**B)** Western blot data in (**A)** were quantified and plotted. (C) Autophagy inhibitor 3-MA diminished the effect of SUMO1 overexpression on protein expression levels of α–SMA, SM22 and SM-MHC. (D) Western blot data in (**A)** were quantified and plotted. **(E)** Autophagy inhibitor 3-MA diminished the effect of increased VSMCs proliferation induced by SUMO1 overexpression. (n = 3/group, *$P < 0.05$, **$P < 0.01$).

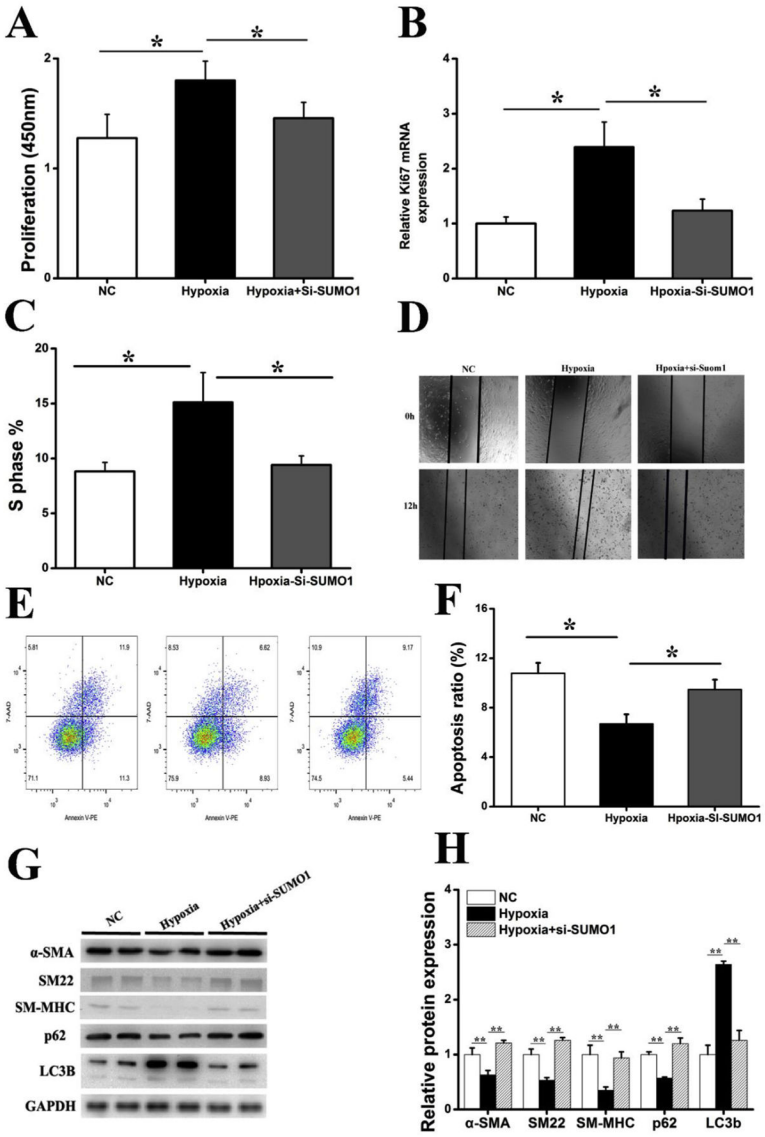

Fig. 7. Knockdown of SUMO1 expression reversed hypoxia-induced proliferation, autophagy, phenotypic switching and migration of PASMCs.

(A) Analysis of cell proliferation of PASMCs with the CCK-8 kit by reading the optical absorbance density at 450 nm. Hypoxia increased PASMCs proliferation, however, the effect was reversed by SUMO1 knockdown. (**B**) SUMO1 knockdown reversed the hypoxia-induced increase of the mRNA expression level of Ki67 (a proliferation marker). (**C**) Flow cytometry analysis to measure the number of cells at the S phase during cell division. Hypoxia significantly increased the cell number at the S phase. SUMO1 knockdown reduced the effect. (**D**) Scratch-wound healing cell migration assay. Hypoxia increased the migration of PASMCs, however, the effect was reversed by SUMO1 knockdown. (E) Flow cytometry analysis to measure the number of apoptotic cells. Hypoxia significantly decreased the level of apoptosis, however, the effect was reversed by SUMO1 knockdown. (F) Analysis of the level of apoptosis. (G) Western blot analysis showing that hypoxia significantly decrease expression levels of α-SMA, SM22, SM-MHC and p62, and a significantly increased

expression level of autophagy marker LC3b in PASMCs. However, the effects were reversed by SUMO1 knockdown. (H) Western blot data in (**G)** were quantified and plotted. (n = 3/group, $*P < 0.05$, $**P < 0.01$).

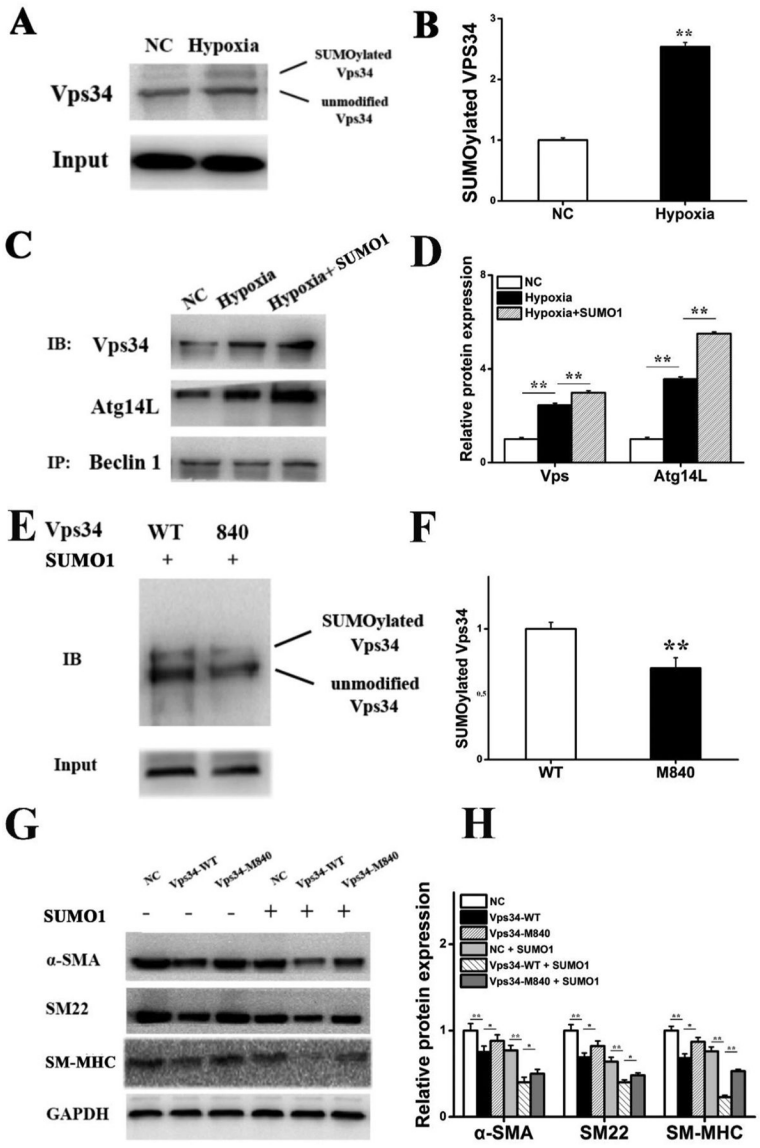

Fig. 8. SUMO1 increases Vps34 SUMOylation involved in the activation of autophagy and hypoxia-induced VSMCs phenotypic switching.

(A) Western blot analysis showed that hypoxia induced binding of SUMO1 to endogenous Vps34 in VSMCs. (B) Western blot data in (**A)** were quantified and plotted. (**C)** Co-immunoprecipitation assays showed that hypoxia increased the Beclin-1/Vps34/ATG14L complex formation, and overexpression of SUMO1 further increased the complex formation Cell extracts were immunoprecipitated with anti-Beclin1 and probed with anti-Vps34, anti-Atg14L. (D) Western blot data in (**C)** were quantified and plotted. (**E)** Vps34 mutant with K840R at the SUMOylation site impaired the binding of SUMO1 to endogenous Vps34 in VSMCs. (F) Western blot data in (**E)** were quantified and plotted. (**G)** Vps34 mutant with K840R significantly increased the protein expression levels of α–SMA, SM22 and SM-MHCas compared to that with Vps34 wild type. (G) Western blot data in (**H)** were quantified and plotted. (n = 3/group, $*P < 0.05$, $**P < 0.01$).

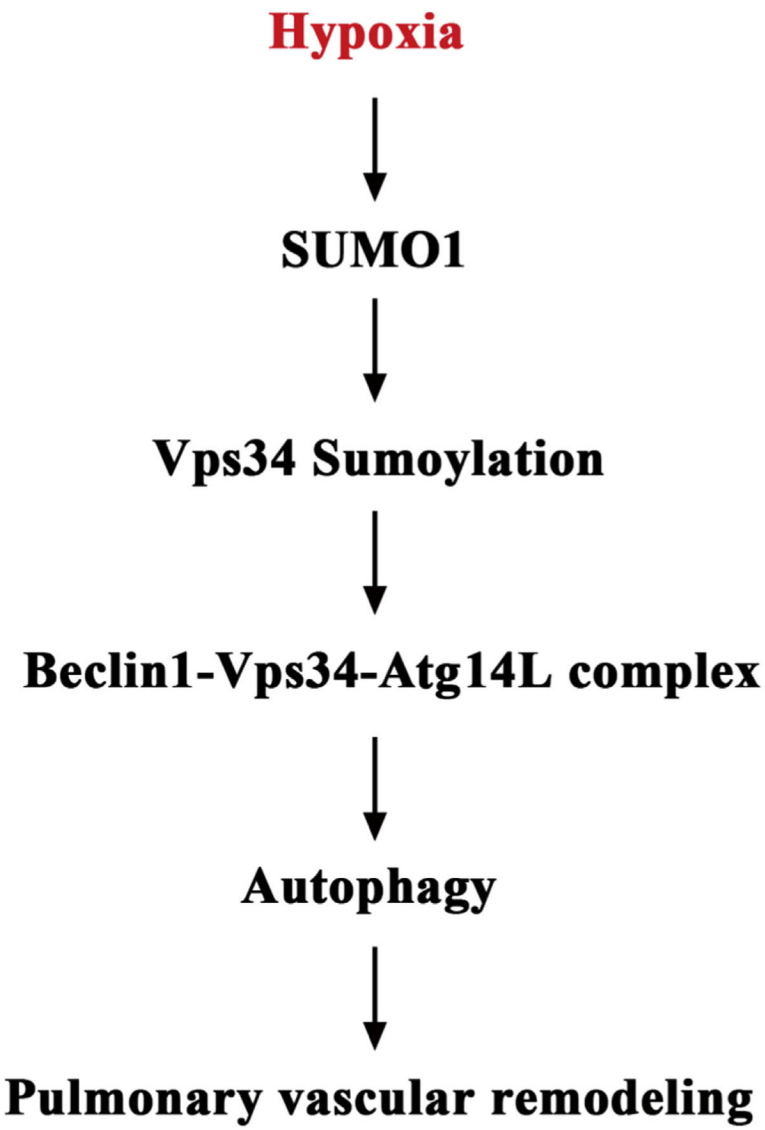

Fig. 9. A schematic working model for a novel SUMO1-regulated mechanism involved in pulmonary vascular remodeling and PAH.

In the hypoxia-induced mouse model for PAH, the expression level of SUMO1 was significantly increased, which induces Vps34 SUMOylation. Vps34 SUMOylation promotes the formation of autophagy initiation complex Beclin-1/Vps34/ATG14L, which induces activation of autophagy, resulting in pulmonary vascular remolding and PAH.